Characterization and Applications of Liquid Crystals in the THz Frequency Range

Ci-Ling Pan *[a], Ru-Pin Pan *[b]
[a] Department of Physics, National Tsing Hua University, Hsinchu, Taiwan 30013, R.O.C;
[b] Department of Electrophysics*, National Chiao Tung University, Hsinchu, Taiwan 30010, R.O.C

ABSTRACT

The applications of liquid-crystal-based devices the sub-millimeter wave or THz (1 THz = 10^{12} Hz) frequency range has blossomed recently. In this paper, we review the methodology for determination of the THz optical constants of nematic liquid crystals, using E7 as an example. To demonstrate potential applications, we report an electrically tuned THz Solc filter.

Keywords: THz, Liquid crystal, birefringent, optical constants, polarization filters, tunable, far Infrared, Solc

1. INTRODUCTION

In the past two decades, THz studies ranging from investigations of ultrafast dynamics in materials to medical, environmental sensing and imaging have been actively explored[1-4]. For these and future applications in THz communication and surveillance, quai-optical components[5] are increasingly in demand. Liquid-crystal-based THz devices are attractive in quasi-optical systems provided LCs exhibit reasonably large birefringence and acceptable transmittance in this increasingly important frequency range can be found. Indeed, several kinds of LC THz devices, e.g., phase shifters[6], birefringent[7, 8], plasmonic[9], and Fabry-Perot filters[10], polarizers[11], phase gratings[12], and Bragg switches[13], have been demonstrated. The present paper reviews the methodology for determination of the THz optical constants of nematic liquid crystals, using E7 as an example. To demonstrate potential applications, we report an electrically tuned THz Solc filter.

2. THZ BIREFRINGENCE AND OPTICAL CONSTANTS OF LIQUID CRYSTALS

For THz LC devices, the knowledge of the extraordinary and ordinary refractive indices, n_e and n_o, as well as the birefringence ($\Delta n = n_e - n_o$) of LCs in the far-infrared (submillimeter wave) or THz frequency range is essential. The preferred technique is THz time-domain spectroscopy or THz-TDS. In the following, we will briefly review the experimental and theoretical methods for extracting the complex optical constants of nematic liquid crystals. The LC mixture E7 (Merck), with wide nematic temperature range (-10ºC~59ºC), was the LC of choice in most of the LC THz devices mentioned above[6-13]., we thus choose E7 as an example to illustrate[14].

2.1 Experimental method

A homogeneously aligned LC cell and a reference cell were prepared in this work. The reference cell was constructed by two optical-grade fused silica windows with thickness of d_1 and d_2, respectively. The LC cell was constructed by sandwiching the LC (E7, Merck) between two windows of the aforementioned types with thickness of d_3 and d_4, respectively. Thickness of the liquid crystal layer was controlled with Mylar spacer and measured by subtracting the substrates thicknesses from the total cell thickness. The LC layer thickness in this work is d_{LC}=0.552±0.002 mm. We achieved homogeneous alignment of the nematic LC by rubbing the polyimide films on the substrates. The temperature of the liquid crystal cell can be varied with an accuracy of ±0.1ºC. Thickness of each of the windows employed was found to be ~3 mm as measured with a micrometer.

To determine the optical constants, A home-made antenna-based THz time-domain spectrometer (THz-TDS) with a collimated beam at the sample position was used [6]. The THz spectrometer was purged with dry nitrogen so that it could be maintained at a relative humidity of (4.0±0.5) %. A schematic of the THz-TDS experiment is shown in Fig. 1. THz-TDS measurements are performed at room temperature (300K). The power spectral S/N ratio is as high as 10^6. Briefly, terahertz pulses generated from femtosecond laser-excited dipole-type antenna fabricated on low-temperature-grown GaAs were collimated by an off-axis paraboloidal mirror and propagated through the sample at normal incidence. The

Emerging Liquid Crystal Technologies VII, edited by Liang-Chy Chien, Proc. of SPIE Vol. 8279, 82790I · © 2012 SPIE · CCC code: 0277-786X/12/$18 · doi: 10.1117/12.914798

transmitted terahertz pulses were focused on another dipole-type antenna that was gated by time-delayed optical probe pulses and oriented to detect terahertz waves that were polarized parallel to the incident terahertz wave polarization. In the experiments, either the reference of LC cell was placed in the THz-TDS at the position where the THz beam was collimated. For measurements of the extraordinary and ordinary indices of refraction, ne and no, we rotate the LC cell such that its director is either perpendicular or parallel to the polarization direction of the incident THz wave.

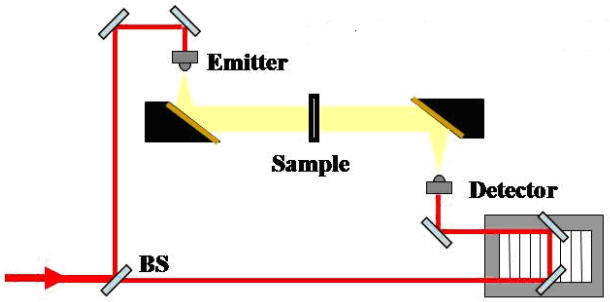

Fig. 1 A general sketch of the home-made THz-TDS system. The arrow indicates laser pulses from a femtosecond Ti: sapphire laser; BS: optical beam splitter.

2.2 Extraction of optical constants

For a monochromatic plane THz wave propagating through the cells at normal incidence (see Fig. 1), we can write the electric field of the THz wave transmitted through the reference cell as

$$E_{ref}(\omega) = E_0(\omega)\tilde{t}_{aw}\tilde{t}_{wa}\cdot\exp\left[-i(\omega/c)\tilde{n}_w(d_1+d_2)\right]\cdot\exp\left[-i(\omega/c)\tilde{n}_a(d_a+\Delta d)\right], \quad (1)$$

Where $E_0(\omega)$ is the electric field of the incident THz wave. The ratios, $\tilde{t}_{aw}=2\tilde{n}_a/(\tilde{n}_a+\tilde{n}_w)$ and $\tilde{t}_{wa}=2\tilde{n}_w/(\tilde{n}_w+\tilde{n}_a)$ are the transmission coefficients of the THz signal from air to the fused silica substrate and from the substrate to air, respectively; $\tilde{n}_w$ and $\tilde{n}_a$ are the refractive indices of the substrate and air. Here, the slight difference in thickness, d_1+d_2 and d_3+d_4 of the reference and LC cells is taken into account by the term $\Delta d = (d_3+d_4)-(d_1+d_2)$; d_a is thickness of a mass of air assumed to have the same value as d_{LC}. Similarly, the electric field of the THz wave passed through the LC cell can be written as

$$E_{LC}(\omega) = E_0(\omega)\tilde{t}_{aw}\tilde{t}_{w-LC}\tilde{t}_{LC-w}\tilde{t}_{wa}\cdot\exp\left[-i(\omega/c)\tilde{n}_w(d_3+d_4)\right]\cdot FP_{LC}(\omega, d_{LC}), \quad (2)$$

where $\tilde{t}_{w-LC}=2\tilde{n}_w/(\tilde{n}_w+\tilde{n}_{LC})$ and $\tilde{t}_{LC-w}=2\tilde{n}_{LC}/(\tilde{n}_{LC}+\tilde{n}_w)$ are the transmission coefficients from fused silica substrate to the LC layer and from the LC layer to the substrate interfaces, respectively. The FP_{LC} parameter is the Fabry-Perot coefficient for multiple reflections of the THz beam in the nematic LC cell, and can be written as

$$FP_{LC}(\omega, d_{LC}) = \sum_{m=0}^{N}\left(\tilde{r}_{LC-w}^{2m}\times\exp\left\{-i(\omega/c)\left[\tilde{n}_{LC}d_{LC}(2m+1)\right]\right\}\right), \quad (3)$$

with a thickness of d_{LC}, and $\tilde{n}_{LC}$ is the complex refractive index of LC. In expressing the transmitted THz wave as in Eqs. (1) and (2), we assumed that the multiple reflections in the substrates can be ignored. Experimentally, this is done by choosing the measurement time window such that the multiple reflections are excluded. Using Eqs.(1) and (2), we can write the transmission coefficient of the LC cell, normalized to that of the reference as

$$\begin{aligned} T(\omega) &= E_{LC}(\omega)/E_{ref}(\omega) \\ &= \tilde{t}_{w-LC}\tilde{t}_{LC-w}\cdot\exp\{-i(\omega/c)\cdot[\Delta d(\tilde{n}_w-\tilde{n}_a)+d_{LC}(\tilde{n}_{LC}-\tilde{n}_a)]\} \\ &\quad\cdot\sum_{m=0}^{N}\tilde{r}_{LC-w}^{2m}\cdot\exp[-i2m(\omega/c)\tilde{n}_{LC}d_{LC}]. \end{aligned} \quad (4)$$

Expressing $\tilde{n}_{LC}$, $\tilde{n}_w$ and $\tilde{n}_a$ into their real and imaginary parts, $\tilde{n}_{LC}=n_{LC}+i\kappa_{LC}$, $\tilde{n}_w=n_w+i\kappa_w$ and $\tilde{n}_a=n_0$, we can write the complex refractive index of LC as following:

$$\begin{aligned} n_{LC} = n_0 + \Big[&\arg\left(T(\omega)\right)-\arg\left(\tilde{t}_{w-LC}\tilde{t}_{LC-w}\exp\left[-\omega\left(\Delta d\kappa_w+d_{LC}\kappa_{LC}\right)/c\right]\right. \\ &\left.\cdot\sum_{m=0}^{N}\tilde{r}_{LC-w}^{2m}\cdot\exp\left(-i2m\tilde{n}_{LC}d_{LC}\omega/c\right)\right)\Big]\cdot c/(\omega\cdot d_{LC})-\Delta d\cdot(n_w-n_0)/d_{LC}, \end{aligned} \quad (5)$$

and

$$\kappa_{LC} = \kappa_w \cdot \Delta d / d_{LC} - \ln\left[|T(\omega)| / \left\{ \left| \sum_{m=0}^{N} \tilde{r}_{LC-w}^{2m} \cdot \exp[-i2m(\omega/c)\tilde{n}_{LC} d_{LC}] \right| \cdot \left| \tilde{t}_{w-LC} \tilde{t}_{LC-w} \right| \right\} \right]$$

$$\cdot c/(\omega \cdot d_{LC}). \qquad (6)$$

Previous studies[6,12] have shown that there is no resonance in the spectral range (0.2~1.2 THz) for either n_e or n_o of E7. It is then expected that its ordinary and extraordinary refractive indices can be fitted by the three-parameter Cauchy formula[15]

$$n_{o,e} = A_{o,e} + B_{o,e}\lambda^{-2} + C_{o,e}\lambda^{-4}. \qquad (7)$$

For several LCs, including E7 at room temperature, Li and Wu[15] have determined the fitting parameters. The birefringence of the liquid crystal can then be calculated using Eq. (7).

.

2.3 Complex Optical Constants of E7

For the range of 0.2~2.0THz, the extraordinary (n_e) and ordinary (n_o) indices of refraction of E7 at 26ºC and its refractive index in the isotropic phase (60ºC) are shown in Fig. 2. Clear anisotropy in nematic phase was observed with n_e = 1.690~1.704 and n_o = 1.557~1.581. The refractive indices decrease slightly with increasing frequency from 0.2 to 2 THz. This general trend is also observed in recent study of the THz birefringence of the homologous series of nematic cyanobiphenyls (CBs) by Vieweg et al.[16]. The corresponding THz birefringence (Δn) of E7 at 26ºC is about 0.130~0.148, and plotted as a function of frequency in Fig. 3. This is comparable to the reported birefringence of E7 in the microwave range (Δn = 0.13~0.15), but somewhat smaller than those in the visible band (Δn = 0.21~0.26). Extinction coefficient of E7 are shown in Fig. 4 with κ_e = 0.010~0.020 and κ_o = 0.028~0.042. In other words, the absorption coefficient for ordinary and extraordinary waves at 1 THz are α_e = 5.001 cm^{-1} and α_o = 15.573 cm^{-1}, respectively. Data shown in Figs. 2 and 4 indicate that there is no sharp absorption feature for E7 in this range. Figure 4 also shows that E7 is dichroic with a dichroic ratio, R = α_o/α_e, being 3.11 at 1 THz.

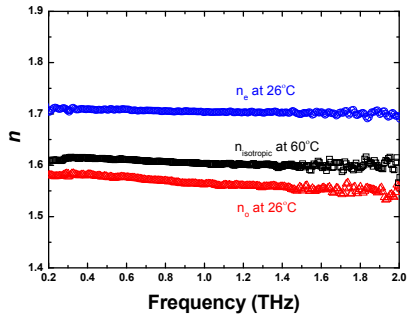

Fig. 2. The real refractive indices of E7 are plotted as functions of frequency. The blue circles and the red triangles are the extraordinary and ordinary refractive indices of E7, n_e and n_o at 26°C, respectively. The black squares are the real refractive indices of E7 in the isotropic phase (at 60°C). The error bars are comparable to or smaller than the symbols.

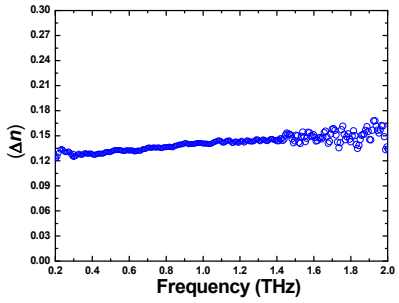

Fig. 3. Frequency dependence of the birefringence of E7 measured at 26°C. The error bars are comparable to or smaller than the symbols.

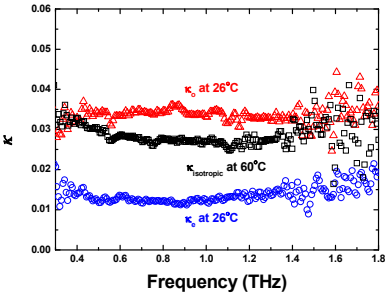

Fig. 4. The imaginary refractive indices of E7 are plotted as functions of frequency. The blue circles and the red triangles are the κ_e and κ_o at 26°C, respectively. The black squares are the imaginary refractive indices of E7 in the isotropic phase (at 60°C). The error bars are comparable to or smaller than the symbols.

2.4 Wavelength-dependence of the optical constants

For comparison, we have organized the refractive indices of E7 reported in the literature from the visible, near infrared, mid-infrared to the millimeter waves together with those of ours in the millimeter and sub-millimeter wave range. This is shown in Fig. 5. The data from the visible to the mid-infrared can be fitted quite well by Eq. (7). The refractive indices in the THz (sub-millimeter wave), millimeter wave and microwave range, however, deviate significantly from the fitting curves. Similarly, the available birefringence data and the fitting curves across the entire spectrum are shown in Fig. 6.

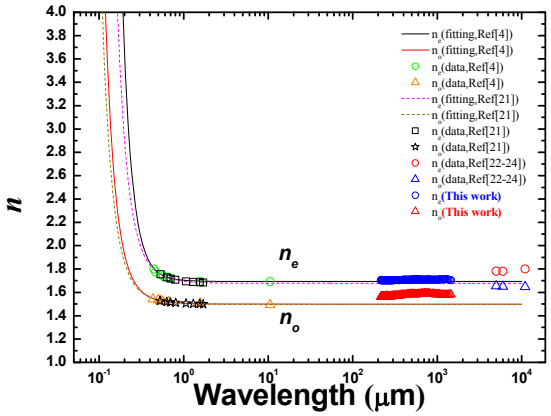

Fig. 5. The refractive indices of E7 reported in the literature from the near infrared, mid-infrared to the millimeter waves together with those of this work in the millimeter and sub-millimeter wave range.

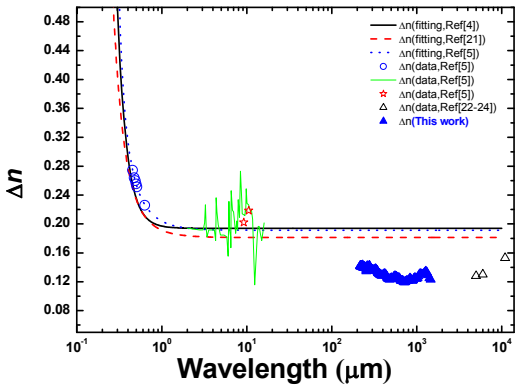

Fig. 6. The birefringence of E7 reported in the literature from the visible, near infrared, mid-infrared to the millimeter waves together with those of this work in the millimeter and sub-millimeter wave range.

The above observations could be qualitatively explained. It is well-known that dispersion could vary significantly near resonances. Cyanobiphenyls, such as 5CB and 7CB, are major components of E7 and 5CB and are known to have broad absorption features near 100, 140 and 165 cm^{-1}, i.e., ~3 to 6 THz.[17] In particular, there is a broad shoulder extending from the sub-THz frequencies to the absorption band near ~ 100 cm^{-1} assigned to the libration of the rigid molecule around its long axis. The far-infrared absorption spectrum of 7CB exhibits similar profiles with absorption bands near ~ 100, 160 and 180 cm^{-1}.[18] Thus we can qualitatively understand the deviation of the THz refractive indices of E7 from Eq. (7), the 3-parameter Cauchy Equation, as it does not take into accounts these far-infrared resonances.

3. ELECTRICALLY TUNED THZ SOLC FILTER

The Lyot[19] and Solc[20] filters are birefringent filters widely employed in the visible and near infrared. These are based on interference of polarized light. We have previously reported a LC based tunable THz Lyot filter[7] with tunable range from 0.388 to 0.564 THz, a fractional tuning range of 40% was also reported. Similarly, a LC Solc filter[21] for which the first central pass-band frequency of the filter can be continuously tuned from 0.176 THz to 0.793 THz was developed by our group. Both devices utilized magnetically controlled birefringence in nematic liquid crystals. Here we describe an electrically tuned THz Solc filter as another example of potential applications of LC devices in the THz frequency range.

3.1 Basic Principles

A typical Solc filter consists of a stack of identical birefringence plates with folded azimuth angles between crossed polarizers or fanned azimuth angles between parallel polarizers. In this work, we have constructed and characterized a THz Solc filter using liquid crystal for the birefringent phase plate. The folded Solc filter design[22] was adopted. It composed of a series of even number of half-wave plates at central frequency f_c between crossed polarizers. Each of the wave plates must be oriented at the azimuth angle ρ and $-\rho$ alternatively with respect to the polarization of incident electromagnetic wave. The central frequency f_c of the filter is given by

$$f_c = \frac{(2m+1)c}{2(n_{eff} - n_o)d}, m = 0, 1, 2, 3 \ldots, \quad (8)$$

Where n_o and n_{eff} are refractive indices of ordinary and effective extraordinary waves, respectively, d is the thickness of each wave plate, and c is the speed of light in vacuum, m is the order of the half-wave plates. The transmittance of the filter is given by $T = \sin^2 2N\rho$. Thus, if the final azimuth angle of polarization is equal to 90° at central frequencies, the light passes through the rear polarizer without any loss of intensity but light at other frequencies will have losses.

3.2 Device Configuration

The electrically tuned LC phase shifter, which is a key element of the design, is shown in Fig 7. Fused silica plates with

an area of 4.5 cm by 2.5 cm were employed as the substrates. The cell is filled with LC, E7 (Merck). We used copper spacers for controlling the thickness of the LC layers to 1.5 mm each. These served as electrodes as well. The distance between two copper spacers is 18mm. The inner surfaces of the plates were coated with DMOAP such that the LC molecules were initially perpendicular to the substrates. One element of a tunable LC THz Solc filter is shown in Fig. 4.3. The propagation direction of THz wave is along the Z-axis and the direction of applied electrical field is tilted at either 22.5° or -22.5° with respect to the X-axis.

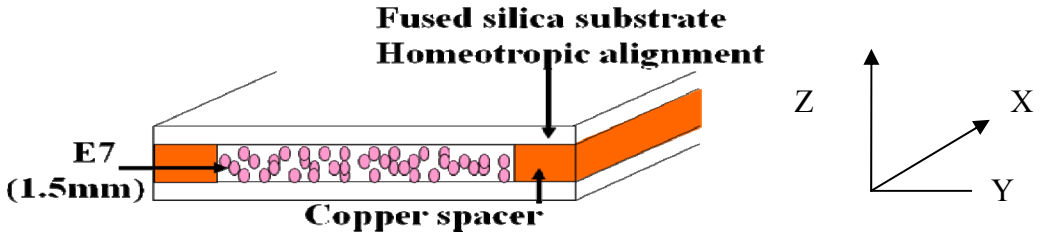

Fig. 7. The schematic diagram of homeotropical alignment LC cell for electrical tuned phase shifter. The cell gap is 1.5mm.

The arrangement of a tunable two folded THz Solc filter based on electric controlled retardation in LC is shown in Fig. 8. The applied electrical field directions have tilting angles 22.5° and - 22.5° with respect to the polarization of input light respectively.

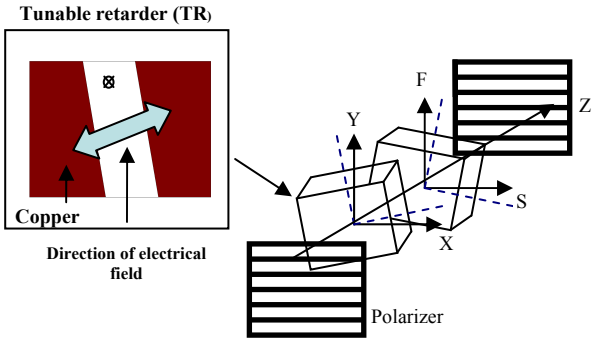

Fig. 8 The schematic diagram of one element in a tunable LC THz Solc filter (left) and the schematic of the two-fold THz Solc filter. The propagation direction of the THz wave is along Z axis. The direction of applied electrical field is tilted with 22.5° or -22.5° referring to X axis.

The arrangement of a tunable dual folded THz Solc filter based on electric controlled retardation in LC is shown in Fig. 8. The applied electrical field directions have tilting angles 22.5° and - 22.5° with respect to the polarization of input light respectively.

The tunable retarder elements are our electrical controlled THz phase shifters, i.e., a homeotropicly aligned LC cell controlled by a pair of copper spacers as electrodes to achieve the desired variable phase retardation, δ(v)

$$\delta(\theta) = 2\pi L \frac{f}{c}\left\{\left[\frac{\cos^2(\theta)}{n_e^{\,2}} + \frac{\sin^2(\theta)}{n_o^{\,2}}\right]^{-\frac{1}{2}} - n_o\right\}, \tag{9}$$

where L is the thickness of LC layer, f is the frequency of the THz waves, c is the speed of light in vacuum, no and ne are the ordinary and extra-ordinary refractive indices of the LC. θ is the angle between the polarization direction of electricomagnetic wave and the pricipal axis of LCs. The theoretical phase retardation can be calculated as we know the no and ne of LC. With positive dielectric anisotropy, the E7 molecules in the bulk of the cell will be reoriented toward the applied electric field if the field is increased beyond the threshold voltage (the Freedericksz transition), $V_{th} = \pi\left(\frac{L}{d}\right)\times\left(\frac{k_3}{\varepsilon_a \varepsilon_0}\right)^{\frac{1}{2}}$, where L is the distance between two electrodes, d is thickness of the NLC layer, and k_3, $\varepsilon_a = \varepsilon_{\parallel} - \varepsilon_{\perp}$, and ε_0 are the bend elastic constant, dielectric anisotropy, and electric permittivity of free space, respectively. We change the applied voltage from 0 to 50V and the threshold voltage (V_{th}) in our work is ~13.4V, with L=18mm, d=1.5mm, $k_3 = 1.71\times10^{-11}$N, and ε_a = 13.8 (from Merck). The applied voltages quoted in this paper are all rms values.

The retardation provided by homeotropic TRs are zero when the LC molecules are parallel to the z-axis and change by varying the applied voltages.

Figure 9 shows the central pass band frequency is tuned from 0.717 to 1.142 THz by changing voltage. The solid curve is theoretical prediction according to the theory and the circles are experimental data.

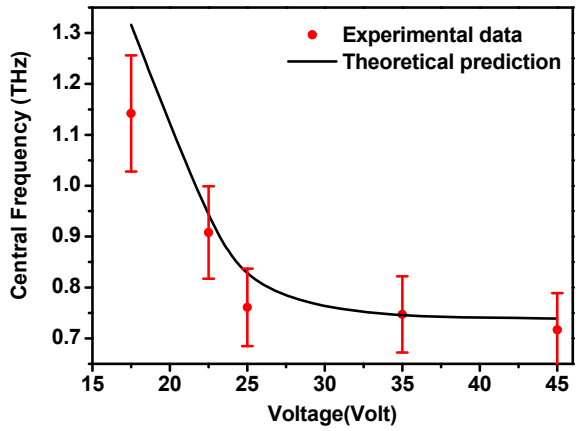

Fig. 9. The central transmitted frequencies of the filter versus applied voltages. The circles are experimental data. The curve is theoretical line

To compare, we have summarized the characteristics of several birefringent LC-based tunable THz filters developed by our group in Table 1.

	Magnetically tuned Solc Filter[8]	**Electrically tuned Solc Filter (this work)**	**Magnetically tuned Lyot Filter[7]**
Tunable Range	0.176 ~ 0.793THz (a fractional tuning range of 350%).	0.717 ~1.142THz (a fractional tuning range of 59%).	0.388~0.564 THz (a fractional tuning range of 40%).
Insertion Loss	~ 5dB	~ 3.7dB	~ 8dB

Table 1 The performance of several types of birefringent LC-based tunable THz filters are compared.

4. SUMMARY

The applications of liquid-crystal-based devices the sub-millimeter wave or THz (1 THz = 10^{12} Hz) frequency range has blossomed recently. In this paper, we review the methodology for determination of the THz optical constants of nematic liquid crystals, using E7 as an example. The extinction coefficient of E7 at room temperature is less than 0.035 and without sharp absorption features in the frequency range of 0.2~2.0 THz. The extraordinary (n_e) and ordinary (n_o) indices of refraction at 26ºC are 1.690~1.704 and 1.557~1.581, respectively, giving rise to a birefringence of 0.130~0.148 in this frequency range. The temperature-dependent (26ºC~70ºC) order parameter extracted from the birefringence data agrees with that in the visible region quite well. Further, the temperature gradients of the THz optical constants of E7 are also determined. The optical constants of E7 in the THz or sub-millimeter wave range are found to deviate significantly from values predicated by the usual extended Cauchy equations used in the visible and near-infrared. To demonstrate potential applications, we report an electrically tuned THz Solc filter. A two-stage folded Solc filter can be electrically tuned with 0.717 ~1.142THz (a fractional tuning range of 59%). The insertion loss of the device is 3.7 dB. This is another example that clearly demonstrates the potential of liquid crystal devices for THz applications.

5. ACKNOWLEDGEMENT

The authors would like to acknowledge and thank members of their group and collaborators, notably Prof. X. –C. Zhang (formerly of RPI, now at Rochester), Profs. M. Tani and M. Hangyo (Osaka and Fukui Universities, respectively), Drs. T.

R. Tsai. C. –Y. Chen, C. –F. Hsieh, H. Y. Wu, C. J. Lin and Mr. Chanshan Yan. Ci-Ling Pan and Ru-Pin Pan were supported by the National Science Council and the Ministry of Education of the ROC under various grants.

REFERENCES

[1] Ferguson, B.and Zhang, X.- C., "Materials for terahertz science and technology," Nature Mater. 1, 26–33 (2002).
[2] Tonouchi, M. "Cutting-edge terahertz technology," Nature Photonics 1, 97-105 (2007)
[3] Ding, Y. J., Hu, Q., Kock, M, and Stutz, C. E., eds., "Special issue on THz materials, devices, and applications," IEEE J. Sel. Top. Quantum Electron. 14, 257-520 (2008).
[4] Zhang, X.-C., Beigang, Rene, and Tanaka, Koichiro, ed., "Special issue on THz Wave Photonics", J. Opt. Soc. Am. B, 25(9), A1-125 (2009).
[5] Goldsmith, P. F., "Quasi-optical techniques," Proc. IEEE, 80, 1729-1741 (1992).
[6] Chen, C.-Y., Hsieh, C.-F., Lin, Y.-F., Pan, R.-P., and Pan, C.-L, "Magnetically tunable room-temperature 2π liquid crystal terahertz phase shifter," Opt. Express, 12, 2630-2635 (2004).
[7] Chen, C.-Y., Pan, C.-L, Hsieh, C.-F., Lin, Y.-F., Pan, R.-P., "Liquid-crystal-based terahertz tunable Lyot filter," Appl. Phys. Lett., 88, 101107 (2006).
[8] Ho, I.-C., Pan, C.-L, Hsieh, C.-F., Lin, Y.-F., Pan, R.-P., "Liquid-crystal-based terahertz tunable Solc filter," Opt. Lett., 33, 1401-1403 (2008).
[9] Pan, C.-L, Hsieh, C.-F., Pan, R.-P., Tanaka, M., Miyamaru, F., Tani, M., and Hangyo, M., "Control of enhanced THz transmission through metallic hole arrays using nematic liquid crystal," Opt. Express, 13, 3921-3930 (2005).
[10] Jewell, S. A., Hendry, E., Issac T. H,.and Sambles, J. R., "Tunable Fabry-Perot etalon for terahertz radiation," New J. Phys., 10, 033012 (2008).
[11] Hsieh, C. F., Lai, Y.-C., Pan, R.-P., and Pan, C.-L., "Polarizing terahertz waves with nematic liquid crystals," Opt. Lett., 33, 1174-1176 (2008).
[12] Lin, C.-J., Li, Y.-T. Hsieh, C.- F., Pan, R.-P. and Pan, C.-L. "Manipulating terahertz wave by a magnetically tunable liquid crystal phase grating," Opt. Express, 16, 2995-3001 (2008).
[13] Wilk, R., Vieweg, N., Kopschinski, O. and Koch, M., "Liquid crystal based electrically switchable Bragg structure for THz waves," Opt. Express, 17, 7377-7382 (2009).
[14] Yang, C. S., Lin, C. J., Pan, R.-P., Que, C., Yamamoto, K., Tani, M., and Pan, C.-L., "The Complex Refractive Indices of the Liquid Crystal Mixture E7 in the THz Frequency Range," J. Opt. Soc. Am. B, 27(9), 1866-1873, (2010).
[15] Li, J., Wu, S.-T., Brugioni, S., Meucci, R. and Faetti, S. "Infrared refractive indices of liquid crystals," J. Appl. Phys., 97, 073501 (2005).
[16] Wilk, R., Vieweg, N., Kopschinski, O. and Koch, M. "Liquid crystal based electrically switchable Bragg structure for THz waves," Opt. Express, 17, 7377-7382 (2009).
[17] Perova, Tatiana S., "Far-infrared and Low-frequency Raman Spectra of Condensed Media," in [Advances in Chemical Physics: Relaxation Phenomena in Condensed Matter], Vol. 87, William Coffey, ed., Wiley, New York, 427-480 (1994),.
[18] Evans, G. J., and Evans, M., "High and low frequency torsional absorptions in nematic K21," J. Chem. Soc. Faraday Trans. 2, 73, 285 – 292 (1977).
[19] Lyot, B., "Un monochromateur grand champ utilisant les interferences en lumiere polarisee, » Ann. Astrophys., **7**, 1593-1595 (1944).
[20] Solc, Ivan, "Birefringent chain filters," J. Opt. Soc. Am. 55, 621–625 (1965).
[21] Ho, I.-C., Pan, C.-L., Hsieh, C.-F., and Pan, R.-P."A Liquid-Crystal-Based Terahertz Tunable Solc Filter," Opt. Lett., 33(13), 1401-1403 (2008).
[22] Yariv A., and. Yeh, P., [Optical Waves in Crystal: Jones Calculus and its Application to Birefringent Optical Systems], Wiley, New York (1984).